Analysis of the Boresight Error Calibration Procedure for Compact Rotary Vane Attenuators

T. Y. Otoshi
Communications Elements Research Section

In previous studies of the compact rotary vane attenuator, the possible error due to stator vane misalignment was not considered. It is shown in this article that even though the stator vanes are misaligned with respect to each other, the boresight error calibration procedure will tend to cause the residual attenuation error to reduce to a type B error which is generally negligible. This analysis applies to conventional as well as to compact rotary vane attenuators.

I. Introduction

At the Jet Propulsion Laboratory it has been recognized for several years that, for purposes of antenna gain and noise temperature calibrations, it is desirable to incorporate a precision rotary vane attenuator (RVA) in the receiving system. The RVA would enable power ratio measurements to be made by RF substitution methods and therefore reduce the present requirements for amplifiers with a high degree of linearity over a large dynamic range. The "front end" of the deep space communication antenna systems operating at 2.3 GHz utilizes WR 430 waveguide components that are assembled inside a Cassegrainian cone housing. Due to the need to keep the waveguide losses to a minimum, the installation of a conventional WR 430 RVA [1.2 to 1.5 m (4 to 5 ft) in length] was not considered practical. The requirements for a shorter low residual loss unit promoted the development of the compact RVA.

In Ref. 1, the results of tests on a test model compact RVA were presented. The test model that was developed in WR 112 waveguide size may be seen in Fig. 1. Excellent agreement was obtained between experimental and theoretical attenuations of the compact RVA which had a total dynamic range of about 30 dB. The theoretical attenuations were computed from a modified law that was derived for compact RVAs. It was shown in Ref. 2 that the same modified law could be used to extend the accurate dynamic attenuation range of a conventional RVA.

In previous studies of the compact RVA, the possible error due to mutual misalignment of stator vanes was not considered. In this article it is shown that it is permissible to neglect the effect of misaligned stator vanes if the described boresight error calibration procedure is used.

II. Modified Law

As derived in Ref. 3, the modified attenuation law for rotary vane attenuators is

$$A_{dB} = -10 \log_{10} [\cos^4 \theta + 10^{-L_{dB}/20} (2 \cos \phi \cos^2 \theta \sin^2 \theta) + 10^{-L_{dB}/10} \sin^4 \theta] \quad (1)$$

where

L_{dB} = attenuation (in decibels) at $\theta = 90$ deg relative to the attenuation at $\theta = 0$ deg

ϕ = phase shift at the rotor output at $\theta = 90$ deg relative to the phase shift at $\theta = 0$ deg

and

$$\theta = \theta_I + \alpha_1 + \alpha_2(\theta_I) \tag{2}$$

where

θ_I = indicated vane angle

α_1 = boresight error (difference between indicated and actual zero-degree vane angle positions)

$\alpha_2(\theta_I)$ = rotary vane angle runout error calibrated relative to $\theta_I = 0$ deg setting. (This error is a function of θ_I, and is due to gearing errors, bearing runout, eccentricities, etc.)

It should be pointed out that the parameters L_{dB} and ϕ are frequency sensitive. However, their values over a broad band of frequencies can be calibrated rapidly and economically by an automatic network analyzer.

The vane angle errors α_1 and $\alpha_2(\theta_I)$ must also be calibrated to ensure that the attenuator follows the law given by Eq. (1). A procedure for calibrating runout error $\alpha_2(\theta_I)$ was previously described in Ref. 3. The method for calibrating the boresight error α_1 will be described in this article.

It is of interest to examine some special cases of the modified law which are important to consider in boresight error calibrations. Analysis of Eq. (1) will reveal that, when $\cos\phi < 10^{-L_{dB}/20}$, the incremental attenuation will become a maximum at a vane angle setting less than 90 deg and have a maximum value greater than L_{dB}. The following relationships apply for $\cos\phi < 10^{-L_{dB}/20}$:

$$(A_{dB})_{max} = A_{dB}\big|_{\theta=\theta_M} = L_{dB} + 10\log_{10}\left(\frac{L - 2\sqrt{L}\cos\phi + 1}{L\sin^2\phi}\right) \tag{3}$$

where

$$L = 10^{L_{dB}/10} \tag{4}$$

$$\theta_M = \cos^{-1}\sqrt{\frac{1 - \sqrt{L}\cos\phi}{L - 2\sqrt{L}\cos\phi + 1}} \tag{5}$$

If $\cos\phi \geqq 10^{-L_{dB}/20}$,

$$(A_{dB})_{max} = L_{dB} \tag{6}$$

$$\theta_M = \pi/2 \tag{7}$$

Figure 2 illustrates the maximum attenuation characteristics of a compact RVA having a value of L_{dB} equal to 30. These curves were generated by the Univac 1108 computer[1] using the modified attenuation law equation. It is of interest to note in the family of curves that when ϕ is in the region $88.2° \leqq |\phi| \leqq 180°$, the maximum attenuation is greater than L_{dB} and will occur at a vane angle setting which is less than 90 deg.

III. Boresight Error Calibration Equations

Substitution of $\sin^2\theta = 1 - \cos^2\theta$ and algebraic manipulations of Eqs. (1) and (2) will lead to the explicit relationship for α_1 given as

$$\alpha_1 = \pm\arccos\sqrt{x} - \theta_I - \alpha_2(\theta_I) \tag{8}$$

where

$$x = \frac{-B \pm \sqrt{B^2 - 4AC}}{2A} \tag{8a}$$

$$A = 1 - \frac{2\cos\phi}{\sqrt{L}} + \frac{1}{L} \tag{8b}$$

$$B = 2\left(\frac{\cos\phi}{\sqrt{L}} - \frac{1}{L}\right) \tag{8c}$$

$$C = \frac{1}{L} - 10^{-A_{dB}/10} \tag{8d}$$

and L was previously defined by Eq. (4).

The plus sign shown in Eq. (8) is chosen if θ_I has a positive value and the minus sign is chosen if θ_I has a negative value. For most cases, the plus sign shown in Eq. (8a) is applicable. The minus sign in Eq. (8a) is used only for special cases where $\cos\phi < 10^{-L_{dB}/20}$ and the vane angle setting falls in the region $\theta_M < |\theta| < \pi/2$, where θ_M is given by Eq. (5).

[1]Computer program written by T. Cullen of the Communications Elements Research Section.

IV. Boresight Error Calibration Procedure

The procedure used to calibrate α_1 of the compact RVA is identical to the one described by Larson (Ref. 4) for conventional RVAs except that measured attenuation values are substituted into the above general α_1 expression derived from the modified law rather than from the $\cos^2\theta$ law. It is necessary that an initial approximate calibration of L_{dB} and ϕ for the compact RVA be obtained. Then, the α_1 calibration procedure is to measure the incremental attenuation at a θ_I setting and substitute the measured value for A_{dB} in Eq. (8d) and compute α_1 from Eq. (8). After computing α_1 values based on measured attenuations at several θ_I settings, an average value of α_1 is computed. For best accuracy, use of data obtained at vane angle settings close to minimum and maximum attenuation regions should be avoided.

Due to the fact that attenuations of a compact RVA deviate significantly from the $\cos^2\theta$ law even at vane angle settings as low as 20 deg, the use of the more general α_1 expression (given by Eq. 8) is recommended for accurate calibration of α_1. As will be shown later, a beneficial outcome of the use of the described calibration procedure is that, if the stator vanes were misaligned with respect to each other, the effect of this misalignment would tend to reduce to a type B (Ref. 5) error which is generally negligible.

Since α_1 is a mechanical misalignment angle, its value can be determined from RF calibrations at a single frequency if internal reflection errors are small. Using 8448-MHz calibrated values of L_{dB} and ϕ and measured attenuation values in the general α_1 expression, average values equal to $(0.0064 \pm 0.0018\, s_{\bar{x}})$ degree and $(-0.178 \pm 0.004\, s_{\bar{x}})$ degree were calibrated for the test model compact RVA (Fig. 1) in the tapered and stepped transition configurations, respectively. The symbol $s_{\bar{x}}$ denotes the calculated standard error based on the number of measurements. The average α_1 value for each configuration was based on measured attenuations at 27 different vane angle settings (between 19 and 80 deg). The differences of the α_1 values for the two transition configurations were attributed mainly to differences in the mechanical alignments of the stator vanes.

V. Effect of Stator Vane Misalignment

The purpose of this analysis is to show that if the stator vanes were misaligned with respect to each other, the α_1 calibration procedure will cause the actual rotor index plane to be established at a plane located approximately midway between the two stator vanes. By establishing the rotor index at this plane, a good fit will result between measured attenuations and the modified law.

Figure 3 depicts the geometry of a general stator vane misalignment case. An arrow at the end of an arc indicates the plane to which the angle is measured with respect to the reference plane located at the beginning of the arc. When the arrow points in a counter-clockwise direction, the angle has a positive value in the equations presented in this analysis. For the general stator vane misalignment geometry of Fig. 3, the equation for theoretical attenuations (relative to minimum attenuation) can be derived as

$$A'_{dB} = -20\log_{10}\left|\cos\theta_v\cos(\theta_v+\theta') + \frac{e^{j\phi}}{\sqrt{L}}\sin\theta_v\sin(\theta_v+\theta')\right| \tag{9}$$

where

$$\theta_v = \theta_I + \alpha_2(\theta_I) + \delta = \theta - \alpha_1 + \delta \tag{10}$$

and

δ = angle between the output stator card and the indicated rotor index plane, rad

θ' = angle of misalignment between stator vanes, rad

Other angles used in this analysis were previously defined by Eq. (2) or can be defined from Fig. 3.

In the absence of internal reflections, the measured attenuation values will closely follow those given by Eq. (9). Substitution of Eq. (9) for A_{dB} in Eq. (8d) and computations of α_1 using Eq. (8) at many vane angle settings will result in an average α_1 value of

$$\bar{\alpha}_1 \simeq \delta + \frac{\theta'}{2} + \bar{\epsilon} \tag{11}$$

where the angles are expressed in radians and

$$\bar{\epsilon} = \frac{1}{N}\sum_{i=1}^{N}\left\{\frac{\left(\frac{\theta'}{2}\right)^2}{\sin 2\theta_i}\left[1 + \frac{2\left(\frac{\cos\phi}{\sqrt{L}}\cos^2\theta_i + \frac{\sin^2\theta_i}{L}\right)}{\cos^2\theta_i - \frac{\cos\phi}{\sqrt{L}}\cos 2\theta_i - \frac{1}{L}\sin^2\theta_i}\right]\right\} \tag{12}$$

and

$$\theta_i = \theta_I + \delta + \frac{\theta'}{2} \tag{13}$$

The derivation of Eq. (12) is involved and therefore presented separately in the Appendix of this article. The approximate formula given by Eq. (11) is useful for showing the relationship between θ' and the calibrated α_1 value. For most compact RVA cases likely to be encountered in practice, the accuracy of the approximate formula for $\bar{\alpha}_1$ will typically be better than 0.001%. The approximate formula becomes inaccurate when vane angle settings approach $\theta = 0$, $\pi/2$, and θ_M, which was defined by Eq. (5).

From the geometry of Fig. 3 and substitution of Eq. (11), one can obtain

$$\alpha_0 = \theta' + \delta - \alpha_1 \approx \frac{\theta'}{2} - \bar{\epsilon} \tag{14}$$

The last expression shows that the new rotor index plane, established by the boresight error calibration procedure, will be located approximately midway between the two stator vanes. If the rotor index were located exactly midway between the stator vanes, the associated attenuation error would be called a type B error (Ref. 5) whose magnitude is very small when θ' is small.

Figure 4 is a sample computer program printout that illustrates the small residual difference between measured and corrected attenuations that results from the boresight calibration procedure even when stator vanes are significantly misaligned. Numerical values as computed from the approximate and exact formulas for α_1 are also compared.

VI. Conclusions

It has been shown that even when the stator vanes of a rotary vane attenuator are misaligned with respect to each other, the boresight error calibration procedure will tend to cause the residual attenuation error to become negligibly small.

A restriction on the analysis is that the effects of internal reflections must be small. If transitions used on the RVA have VSWRs of 1.02 or less, the effects of internal reflections can be neglected.

References

1. Otoshi, T. Y., "RF Calibration Techniques: A Precision Compact Rotary Vane Attenuator," in *The Deep Space Network*, Space Programs Summary 37-62, Vol. II, pp. 81–87. Jet Propulsion Laboratory, Pasadena, Calif., Mar. 31, 1970.
2. Otoshi, T. Y., "Improved RF Calibration Techniques: Rotary Vane Attenuator Calibrations," in *The Deep Space Network*, Space Programs Summary 37-60, Vol. II, pp. 41–43. Jet Propulsion Laboratory, Pasadena, Calif., Nov. 30, 1969.
3. Otoshi, T. Y., and Stelzried, C. T., "Improved RF Calibration Techniques: WR 430 Waveguide Precision Rotary Vane Attenuator Calibration," in *The Deep Space Network*, Space Programs Summary 37-46, Vol. III, pp. 73–82. Jet Propulsion Laboratory, Pasadena, Calif., July 31, 1967.
4. Larson, W., "Analysis of Rotation Errors of a Waveguide Rotary Vane Attenuator," *IEEE Trans. Instrumentation and Measurements*, Vol. IM-12, pp. 50–52, Sept. 1963.
5. Larson, W., "Analysis of Rotationally Misaligned Stators in the Rotary Vane Attenuator," *IEEE Trans. Instrumentation and Measurements*, Vol. IM-16, pp. 225–231, Sept. 1967.

Appendix

Derivation of Approximate α_1 Formula for Misaligned Stator Vane Case

Derivation of the approximate formula given by Eq. (12) is laborious and the details are involved. However, due to the importance of the approximate formula and the insight it provides for stator vane misalignment analysis, details of the derivation are presented here. The same analysis applies to conventional as well as to compact RVAs.

It was found from studying numerical results from a computer that substitutions of Eq. (9) into Eqs. (8a) and (8) generally produced the result

$$\alpha_1 = \delta + \frac{\theta'}{2} + \epsilon \tag{15}$$

where ϵ is very small compared to θ'. It is difficult to prove this result analytically from direct analysis of Eq. (8). However, an approximate formula for ϵ was derived by use of the following indirect but equivalent method. Let the expression for α_1 as given by Eq. (15) be substituted into Eq. (10). Then, further substitution of Eq. (10) into Eq. (9) results in

$$A'_{dB} = -10\log_{10}\left|\cos\left(\theta - \frac{\theta'}{2} - \epsilon\right)\cos\left(\theta + \frac{\theta'}{2} - \epsilon\right) + \frac{e^{j\phi}}{\sqrt{L}}\sin\left(\theta - \frac{\theta'}{2} - \epsilon\right)\sin\left(\theta + \frac{\theta'}{2} - \epsilon\right)\right|^2 \tag{16}$$

From use of trigonometric identities and the assumptions that θ' and ϵ are small radian angles, the following approximate formula can be derived:

$$A'_{dB} \simeq -10\log_{10}\left|\left(\cos^2\theta + \frac{e^{j\phi}}{\sqrt{L}}\sin^2\theta\right) + \left(z - \frac{e^{j\phi}}{\sqrt{L}}[z + 2k]\right)\right|^2 \tag{17}$$

where

$$z = \epsilon\sin 2\theta - k \tag{18}$$

$$k = \left(\frac{\theta'}{2}\right)^2 \tag{19}$$

As was previously described, the exact procedure for determining α_1 is to substitute Eq. (16) into Eq. (8d) and compute α_1 from Eq. (8). The approximate equivalent procedure is to equate Eq. (17) to the modified law; then solve for ϵ and then substitute the derived expression for ϵ back into Eq. (15).

As a result of equating Eq. (17) to the modified attenuation law which can also be expressed as

$$A_{dB} = -10\log_{10}\left|\cos^2\theta + \frac{e^{j\phi}}{\sqrt{L}}\sin^2\theta\right|^2 \tag{20}$$

a quadratic equation[2] of the form

$$az^2 + bz + c = 0 \tag{21}$$

is obtained. For compact and conventional RVAs the condition $b^2 >> 4ac$ nearly always applies and, therefore, the approximate solution of the quadratic equation $z \simeq -c/b$ can be used. Using this approximation and omitting higher order terms and then solving for ϵ yields the expression

$$\epsilon \simeq \frac{\left(\frac{\theta'}{2}\right)^2}{\sin 2\theta}\left[1 + \frac{2\left(\frac{\cos\phi}{\sqrt{L}}\cos^2\theta + \frac{\sin^2\theta}{L}\right)}{\cos^2\theta - \frac{\cos\phi}{\sqrt{L}}\cos 2\theta - \frac{1}{L}\sin^2\theta}\right] \tag{22}$$

where ϵ, θ' are expressed in radians. For convenience of computations, one can substitute $\theta = \theta_I + \delta + \theta'/2$ in Eq. (22) and sacrifice only a small loss of accuracy.

[2]If u and v are general complex expressions and $|u + v|^2 = |u|^2$, then the condition $|v|^2 + 2\,\mathrm{Re}\,[uv^*] = 0$ must hold. The symbol (*) denotes complex conjugate.

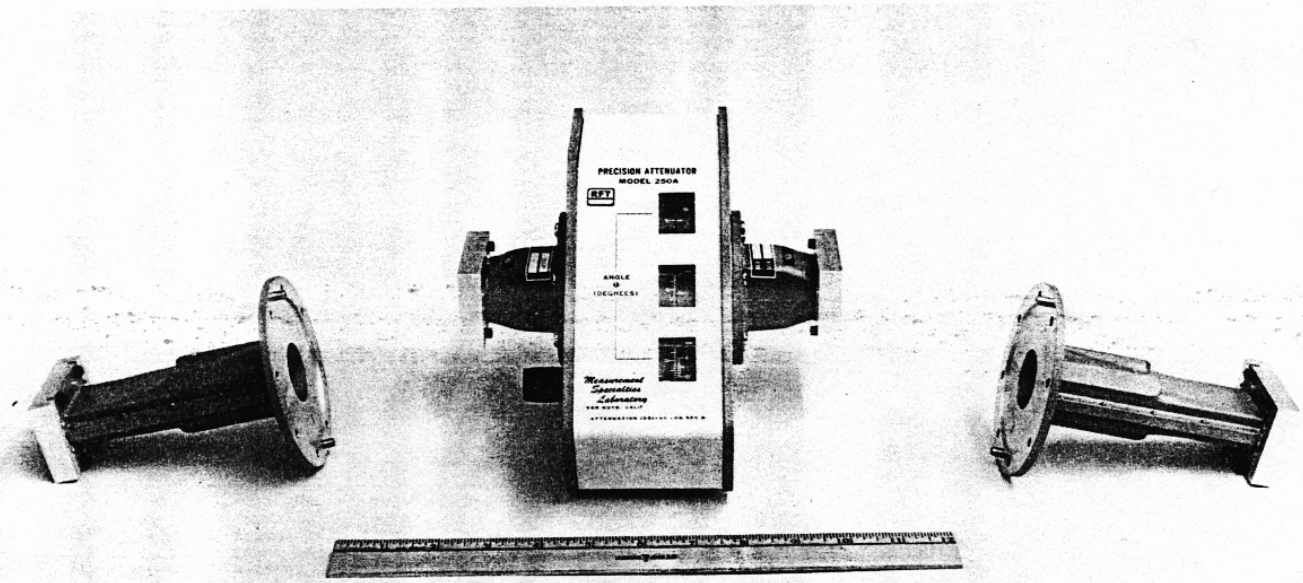

Fig. 1. Test model compact RVA shown with interchangeable transitions

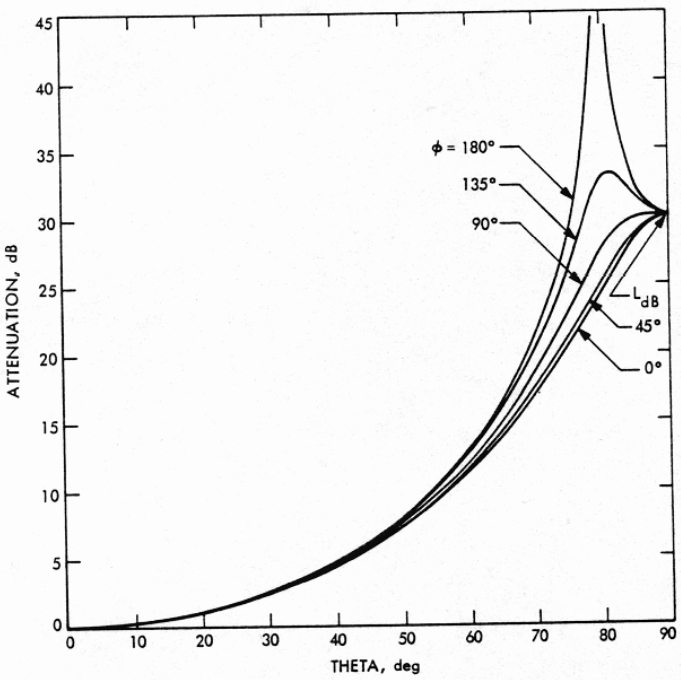

Fig. 2. Compact RVA attenuator curves for $L_{dB} = 30$

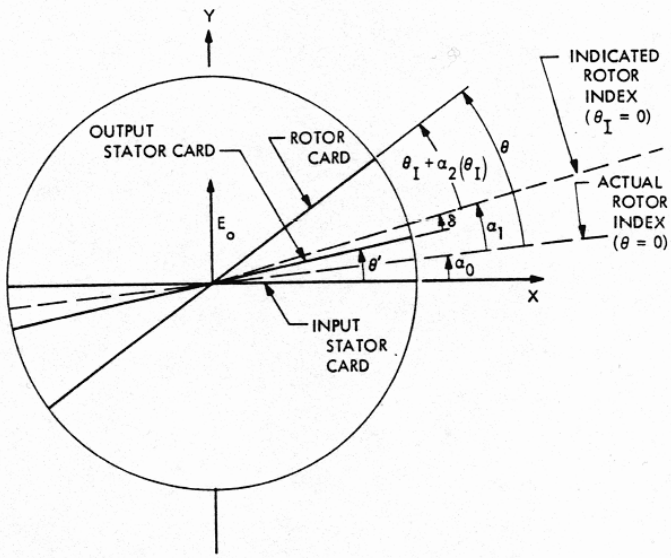

Fig. 3. Geometry for a general rotor and stator vane misalignment case

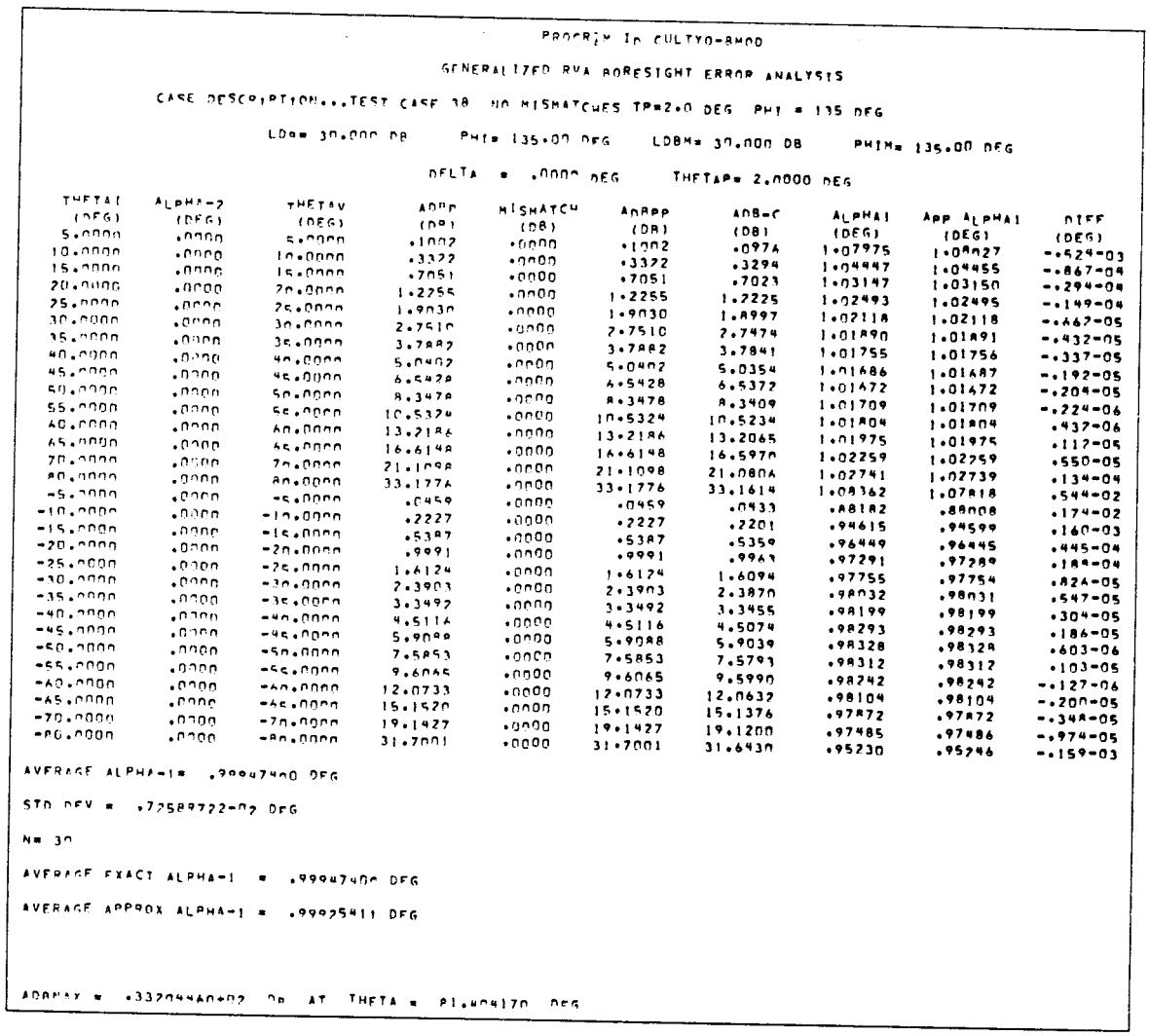

PROGRAM ID CULTYO-8M00

GENERALIZED RVA FORESIGHT ERROR ANALYSIS

CASE DESCRIPTION...TEST CASE 38 NO MISMATCHES TP=2.0 DEG PHI = 135 DEG

LDB= 30.000 DB PHI= 135.00 DEG LDBM= 30.000 DB PHIM= 135.00 DEG

DELTA = .0000 DEG THETAP= 2.0000 DEG

THETAI (DEG)	ALPHA-2 (DEG)	THETAV (DEG)	ADBP (DB)	MISMATCH (DB)	ADBPP (DB)	ADB-C (DB)	ALPHA1 (DEG)	APP ALPHA1 (DEG)	DIFF (DEG)
5.0000	.0000	5.0000	.1002	.0000	.1002	.0974	1.07975	1.08027	-.524-03
10.0000	.0000	10.0000	.3322	.0000	.3322	.3294	1.04447	1.04455	-.867-04
15.0000	.0000	15.0000	.7051	.0000	.7051	.7023	1.03147	1.03150	-.294-04
20.0000	.0000	20.0000	1.2255	.0000	1.2255	1.2225	1.02493	1.02495	-.149-04
25.0000	.0000	25.0000	1.9030	.0000	1.9030	1.8997	1.02118	1.02118	-.462-05
30.0000	.0000	30.0000	2.7510	.0000	2.7510	2.7474	1.01890	1.01891	-.432-05
35.0000	.0000	35.0000	3.7882	.0000	3.7882	3.7841	1.01755	1.01756	-.337-05
40.0000	.0000	40.0000	5.0402	.0000	5.0402	5.0354	1.01686	1.01687	-.192-05
45.0000	.0000	45.0000	6.5428	.0000	6.5428	6.5372	1.01672	1.01672	-.204-05
50.0000	.0000	50.0000	8.3478	.0000	8.3478	8.3409	1.01709	1.01709	-.224-06
55.0000	.0000	55.0000	10.5324	.0000	10.5324	10.5234	1.01804	1.01804	.437-06
60.0000	.0000	60.0000	13.2186	.0000	13.2186	13.2065	1.01975	1.01975	.117-05
65.0000	.0000	65.0000	16.6148	.0000	16.6148	16.5970	1.02259	1.02259	.550-05
70.0000	.0000	70.0000	21.1098	.0000	21.1098	21.0804	1.02741	1.02739	.134-04
80.0000	.0000	80.0000	33.1776	.0000	33.1776	33.1614	1.04362	1.07818	.544-02
-5.0000	.0000	-5.0000	.0459	.0000	.0459	.0433	.88182	.88008	.174-02
-10.0000	.0000	-10.0000	.2227	.0000	.2227	.2201	.94615	.94599	.160-03
-15.0000	.0000	-15.0000	.5387	.0000	.5387	.5359	.96449	.96445	.445-04
-20.0000	.0000	-20.0000	.9991	.0000	.9991	.9963	.97291	.97289	.184-04
-25.0000	.0000	-25.0000	1.6124	.0000	1.6124	1.6094	.97755	.97754	.824-05
-30.0000	.0000	-30.0000	2.3903	.0000	2.3903	2.3870	.98032	.98031	.547-05
-35.0000	.0000	-35.0000	3.3492	.0000	3.3492	3.3455	.98199	.98199	.304-05
-40.0000	.0000	-40.0000	4.5116	.0000	4.5116	4.5074	.98293	.98293	.186-05
-45.0000	.0000	-45.0000	5.9088	.0000	5.9088	5.9039	.98328	.98328	.603-06
-50.0000	.0000	-50.0000	7.5853	.0000	7.5853	7.5793	.98312	.98312	.103-05
-55.0000	.0000	-55.0000	9.6065	.0000	9.6065	9.5990	.98242	.98242	-.127-06
-60.0000	.0000	-60.0000	12.0733	.0000	12.0733	12.0639	.98104	.98104	-.200-05
-65.0000	.0000	-65.0000	15.1520	.0000	15.1520	15.1376	.97872	.97872	-.348-05
-70.0000	.0000	-70.0000	19.1427	.0000	19.1427	19.1200	.97485	.97486	-.974-05
-80.0000	.0000	-80.0000	31.7001	.0000	31.7001	31.6930	.95230	.95246	-.159-03

AVERAGE ALPHA-1= .9994740 DEG

STD DEV = .72589722-02 DEG

N= 30

AVERAGE EXACT ALPHA-1 = .9994740 DEG

AVERAGE APPROX ALPHA-1 = .99925411 DEG

ADBMAX = .33204440+02 DB AT THETA = 81.404170 DEG

Fig. 4. Sample printout of computer program showing relationship of θ' to α_1